Reaction Chemistry & Engineering

Continuous hydrothermal leaching of LiCoO2 cathode materials by using citric acid

Journal:	*Reaction Chemistry & Engineering*
Manuscript ID	RE-ART-07-2020-000286.R1
Article Type:	Paper
Date Submitted by the Author:	30-Jul-2020
Complete List of Authors:	Zheng, Qingxin; Tohoku University Graduate School of Engineering School of Engineering, Department of Chemical Engineering Shibazaki, Kensuke; Tohoku University, Faculty of Environmental Studies Ogawa, Tetsufumi; Tohoku University, Faculty of Environmental Studies Kishita, Atsushi; Tohoku University, Department of Chemical Engineering Hiraga, Yuya; Research Center of Supercritical Fluid Technology, Tohoku University Nakayasu, Yuta; Tohoku University, Watanabe, Masaru; Tohoku University Graduate School of Engineering School of Engineering, Department of Chemical Engineering

ARTICLE

Continuous hydrothermal leaching of $LiCoO_2$ cathode materials by using citric acid

Received 00th January 20xx,
Accepted 00th January 20xx

DOI: 10.1039/x0xx00000x

Qingxin Zheng,*[a] Kensuke Shibazaki,[b] Tetsufumi Ogawa,[b] Atsushi Kishita,[a] Yuya Hiraga,[a] Yuta Nakayasu,[c] Masaru Watanabe*[a]

The first running of continuous hydrothermal leaching of lithium-ion battery cathode materials, $LiCoO_2$, was performed using citric acid as the leachant at 200 °C. The flow system was specially designed and customized. Prior to the hydrothermal leaching experiments, a three-layer model was used to predict the flow state in this flow system, and a cold flow test using two kinds of flow lines was performed to determine the conditions in the preliminary experiments. Finally, the pulp density of the slurry and the flow rate were set to 10 g/L and 30 ml/min, respectively, for the continuous hydrothermal leaching experiments. At 60 min after the start of slurry feeding, the leaching efficiency of Li and Co reached 81.3% and 92.7%, respectively, and can continue to increase with the extension of time. The successful running indicated that the process of hydrothermal leaching is feasible and promising to be applied in practice. Meanwhile, a problem of acid corrosion caused by the use of citric acid during this process was revealed and is expected to be resolved using the inner coating materials with high acid corrosion resistance or the organic acids with low or no acid corrosion as the leachant.

1 Introduction

Due to high voltage, high stability, long life, and light weight, lithium-ion batteries (LIBs) are being widely applied from portable electronic devices to electric vehicles.[1] To meet the global demand for power sources, the manufacture of LIBs is increasing greatly,[2] followed by a huge consumption of various cathode materials used in LIBs and a massive generation of spent LIBs.[3-5]

LIB cathode materials are usually composed of lithium-contained oxides of transition metals, such as $LiCoO_2$, $LiNiO_2$, $LiMn_2O_4$, $LiFePO_4$, $LiMnPO_4$, $LiCoPO_4$, and their mixtures.[4] Metal components in LIBs need a stable supply to meet the increasing consumption; however, some of them are mainly produced from limited countries or geographically remote areas and thus have unstable supplies caused by geopolitical issues.[6, 7] For example, about 70% of Co are produced by Congo (59%), Australia (5%), and Russia (7%).[8] Mining supply of metals, such as Li and Co, is predicted to reach their limits and will be exceeded by the demand soon. On the other hand, spent LIBs are regarded as a kind of hazardous solid wastes, which would bring a tremendous burden on the environment and resource conservation.[2] Therefore, efficient recovery of valuable metals (e.g., Li, Co, Ni, and Mn) from spent LIBs under a mild condition will be essential to conserve natural resources, reduce the environmental problems, keep resource stability and security, and bring economic benefits.[9] As the first type of commercialized cathode material, $LiCoO_2$ has been widely employed in most commercial LIBs, and recently, the quantity of discarded $LiCoO_2$ is increasing regularly and continuously.[10] Compared with other LIB materials, spent $LiCoO_2$ is always regarded as a worthy target for recycling because it is rich in Li and Co.[11]

The hydrometallurgy is one of the conventional methods for recovering metal components from spent LIBs in lab and industry, composed of acid leaching in the first step and separation in the second step.[12, 13] In the leaching stage, spent LIB cathode materials, such as $LiCoO_2$, $LiNiO_2$, and $LiMn_2O_4$, are converted to an aqueous solution of mixed metal ions. A traditional and well-known process is leaching metal ions with mineral or inorganic acid (e.g., sulfuric acid or nitrate acid) in non-pressurized hot water.[14] Meanwhile, chemical reductants (e.g., H_2O_2, $NaHSO_3$, or $Na_2S_2O_3$)[15] are added to improve leaching efficiency and lower the required concentration of acids. Due to the drawbacks in terms of high-concentration inorganic acids, consumption of reductants, batch-style apparatus, long time, and strong acid corrosion, the traditional leaching process always brings severe environmental pollution and economic burden. Therefore, making this process greener and more environmentally-friendly step by step is attracting increasing attention.

[a] Research Center of Supercritical Fluid Technology, Department of Chemical Engineering, Graduate School of Engineering, Tohoku University, 6-6-11 Aoba, Aramaki, Aoba-ku, Sendai, 980-8579 Japan
[b] Faculty of Environmental Studies, Tohoku University, 6-6-11 Aoba, Aramaki, Aoba-ku, Sendai, 980-8579 Japan
[c] Frontier Research Institute for Interdisciplinary Sciences, Tohoku University, 6-6-11-406 Aoba, Aza, Aramaki, Aoba-ku, Sendai 980-8578 Japan
* masaru.watanabe.e2@tohoku.ac.jp (M. Watanabe); qingxin.zheng.a2@tohoku.ac.jp (Q. X. Zheng).

Electronic Supplementary Information (ESI) available: Information of the linear fitting lines for the plots used in kinetic study. See DOI: 10.1039/x0xx00000x

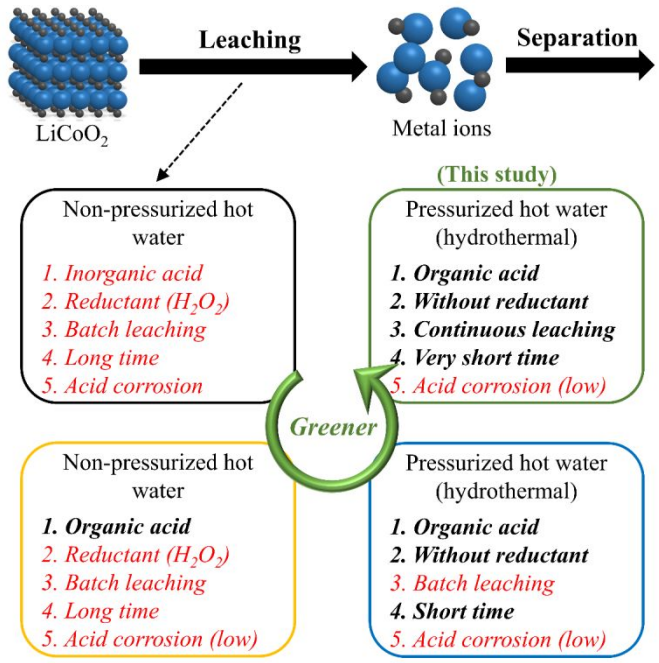

Scheme 1 The green progress of acid leaching process for $LiCoO_2$. The words marked in red color are the problems to be resolved.

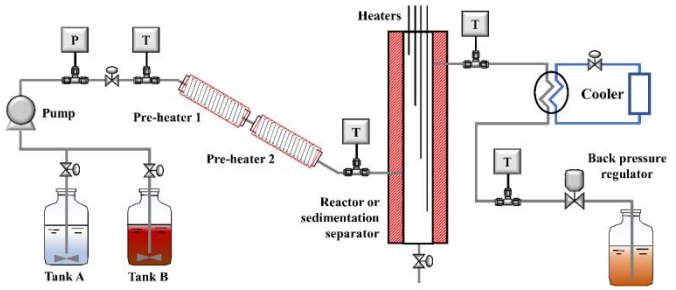

Scheme 2 The schematic diagram of the continuous hydrothermal leaching system.

As shown in **Scheme 1,** looking for alternatives to inorganic acids is the first stage in the green progress of the acid leaching process for $LiCoO_2$. Compared to inorganic acids, organic acids are milder with lower acid corrosion and pollution. Until now, there have been plenty of reports on leaching metal ions from spent LIB cathode materials using organic acids as the leachant, such as succinic acid,[16] malic acid,[17] aspartic acid,[17] citric acid (H_3Cit),[18-20] acetic acid,[21] lactic acid,[22] tartaric acid,[23] oxalic acid,[24] glycine,[25] and so on. These achievements have proved that organic acids could displace inorganic acids for the acid leaching process. However, the reductants are still indispensable to reduce the transition metal ions from the high to low state.[18] For example, without the reductants, the leaching efficiencies of Li and Co decreased significantly, no matter the use of inorganic or organic acids.[6, 7, 17, 26]

Up to now, two feasible paths have been reported to avoid the consumption of additional reductant. The one is leaching with ascorbic acid.[27] During the process, ascorbic acid plays the roles of both leachant and reductant. Another one was proposed in 2017, using pressurized hot water to leach Li and Co from $LiCoO_2$ with H_3Cit, and the process was also called by 'hydrothermal leaching'.[26] Without using any reductant like H_2O_2, hydrothermal leaching with H_3Cit (0.4 mol/L) achieved a leaching efficiency of 94% for both Li and Co at 200 °C for 10 min.[26] This good performance was attributed to that H_3Cit supplies proton, forms a soluble complex with Co, and shows reducibility even though H_3Cit does not work as a reductant below 100 °C. Different from the traditional leaching process using non-pressurized hot water, the temperature of the hydrothermal leaching process is not limited by the boiling point of water at 100 °C. The use of high temperature greatly accelerates the reaction, shortens the reaction time, and decreases the required concentration of acid.[28] With a lower concentration of acids, no consumption of reductants, and higher reaction rate, hydrothermal leaching is more efficient and environmentally-friendly than the traditional leaching method, although organic acid is used in each of them.

One of the next targets in the green progress is developing the leaching apparatus from batch to continuous flow system, which can enhance the productivity, reduce the processing time, improve the quality, lower reagent and power consumption, save the costs, facilitate the scale-up, and move forward to the industrial application.[29, 30] To our knowledge, continuous acid leaching of metal components from LIB cathode materials using a flow system has never been achieved in any conventional hydrometallurgy process, due to possible reasons such as the long reaction time and severe acid corrosion caused by the use of inorganic acids or high-concentration organic acids. Performed in pressurized hot water with low-concentration organic acids, the method of hydrothermal leaching becomes one of the promising candidates to realize the continuous leaching, but its development is just in the initial stage and the device is currently limited to the batch-style apparatus with a small scale. Therefore, at the current stage, a flow system, in which the hydrothermal leaching can be performed continuously, is urgently demanded.

In this study, we applied a specifically designed and customized flow system to perform the continuous hydrothermal leaching of $LiCoO_2$ using H_3Cit as the leachant for the first time. The preliminary conditions such as pulp density of the slurry and flow rate were determined based on the results of a three-layer model and a cold flow test without heating. During the first running of continuous hydrothermal leaching experiments, the experimental conditions were given in detail, the flow system was modified, the results of leaching efficiency were obtained, and problems such as acid corrosion as well as feasible resolutions were considered.

2 Experimental

2.1 Reactants

Commercial LIB cathode material, $LiCoO_2$ (>98%, STREM Chemicals, layered rocksalt), and H_3Cit (>99.5%, FUJIFILM Wako Pure Chemical), were purchased and used without further purification or treatment. Based on the light scattering results (**Fig. S1**), the diameter of $LiCoO_2$ particles mainly distributed in the range of 5–40 μm. Ultra-pure water was supplied by a

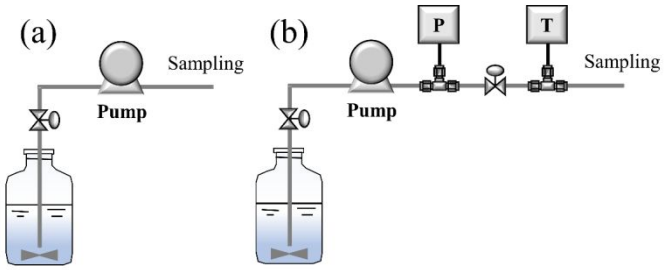

Scheme 3 Schematic diagrams of (a) flow line A and (b) flow line B for the cold flow test.

distillation apparatus (WG-220, Yamato Co.) and had a conductivity of 5.5 μS·m^{-1}.

2.2 Apparatus

Scheme 2 shows the schematic diagram of a laboratory-scale continuous hydrothermal leaching system. Two feeding tanks (tank A and B, with a stirrer inside), a slurry pump (JASCO Corporation, PU-2100S), two pre-heaters (pre-heater 1 and 2, twined by the piping tube and wrapped by the heat insulator), a reactor or sedimentation separator (SUS304, 1 inch; twined by four coil heaters and wrapped by the heat insulator), a cooler (SIBATA), a back-pressure regulator (JASCO, BP-2080-M), and a product collector, were connected in series. The lines between feeding tanks and the slurry pump were made by Teflon, and the other piping tubes (GL Sciences, 1/8 inch) and connectors (Swagelok) were made by stainless steel SUS316. The heaters (Hakko Electric, DGT0010) in the reactor from top to bottom were denoted as heater 1, heater 2, heater 3, and heater 4, respectively. In the reactor, the liquid and solid products were separated from the top and bottom, respectively. To restrain the sedimentation of solid particles in the slurry, the position of the feeding tank is higher than the collector. Many thermocouples in the system were used to monitor the temperature conditions and control the heaters accurately.

2.3 Cold flow test

Prior to the hydrothermal leaching experiment, a flow test without heating (or cold flow test) was conducted to explore the initial conditions, such as flow rate and pulp density. Here, two flow lines (A and B) were used for flowing test, as shown in **Scheme 3**. In a typical experiment, tank A and B were filled with pure water and a mixing slurry of $LiCoO_2$/water (pulp density: 1–50 g/L), respectively. First, pure water was pumped into the system with a specific flow rate (10 or 30 ml/min). After confirming that the water reached the outlet, the supplying of the pure water was stopped and the slurry supplying began. After continuous flowing for 10 min, sampling was started and performed 6 times with an interval of 5 min. After evaporating the water, the solid product contained in the recovered solution could be obtained. The pulp density of the recovered solution was calculated by the weight of the slurry and the weight of the solid product contained in the slurry. Based on the pulp density of each recovered solution, the stability of flowing or pumping was judged and evaluated.

2.4 Continuous hydrothermal leaching of $LiCoO_2$ with H_3Cit

A 0.4 mol/L H_3Cit aqueous solution (>2 L) was prepared and placed in tank A. A slurry (pulp density: 10 g/L) was prepared by mixing 20 g of $LiCoO_2$ with 1980 g of a 0.4 mol/L H_3Cit aqueous solution, and was placed into tank B. In a typical experiment, pure water was pumped to the system with a flow rate of 30 ml/min, and the system pressure was controlled to 20 MPa by the back-pressure regulator. In consideration of safety, the pressure was increased by 5 MPa at a time. After confirming that the system pressure was maintained and there was no liquid leakage from the system, heating was started. In this study, the leaching temperature was 200 °C, and the setting temperatures of pre-heaters and heaters were increases step by step, as shown in **Table 1**. The setting temperature of the heater at the bottom of the reactor was lower than that at the top. This is to restrain the density difference of the liquid due to the difference in temperature, which can generate convection in the reactor and reduce the separation performance, promote the precipitation of the unleached materials, and prevent the blocking at the outlet of the reactor.

After the temperature became unchanged, the supply of pure water was stopped, and the H_3Cit aqueous solution was supplied into the system from tank A. After about 15 min, the water in the system was completely displaced by the H_3CIt solution. After confirming that the pressure was maintained, there was no leakage, and the heating was stable, the supply of the H_3Cit aqueous solution was stopped, and the slurry supplying was started. During the experiment, the slurry in the feeding tank was stirred at a speed of 600–800 rpm using a 4-blade stirrer (AS ONE, SM-101) to suppress solid-liquid separation. Sampling was started after the slurry was fed for 15 min, and performed 10 times with an interval of 5 min.

Table 1 Setting temperature for each pre-heater or heater at different steps*.

	Step 1	Step 2	Step 3	Step 4	Step 5	Step 6
Pre-heater 1	150	180	180	200	200	200
Pre-heater 2	150	180	180	200	200	200
Heater 1	100	125	150	180	200	200
Heater 2	100	125	150	180	200	200
Heater 3	70	100	125	150	180	195
Heater 4	40	80	100	120	150	190

*: The preheaters or heaters were heated step by step to the specific temperatures.

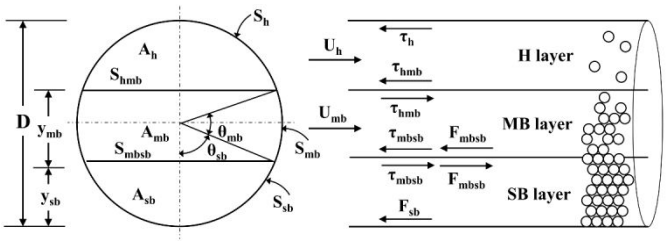

Scheme 4 Schematic diagram of the three-layer model. Here, H layer is a heterogeneous flow; MB layer is a moving bed; SB layer is a stationary bed; D is the pipe diameter; y_{mb} and y_{sb} are the heights of the MB and SB layer, respectively; A_h, A_{mb}, and A_{sb} are the cross-sectional areas occupied by the H, MB, and SB layers, respectively; S_h, S_{mb}, and S_{sb} are the contact surface of pipe wall with the H, MB, and SB layer, respectively; S_{hmb} is the interface between the H and MB layers; S_{mbsb} is the interface between the MB and SB layers; θ_{mb} and θ_{sb} are the central angles associated with y_{mb} and y_{sb}; U_h and U_{mb} are the mean velocities of the H and MB layer, respectively; τ_h and τ_{hmb} are the upper layer shear stress and the interfacial shear stress acting on S_h and S_{hmb}, respectively; τ_{mbsb} and F_{mbsb} are the hydrodynamic shear stress and the dry friction force acting on S_{mbsb}, respectively; F_{sb} is the dry friction force acting on S_{sb}.

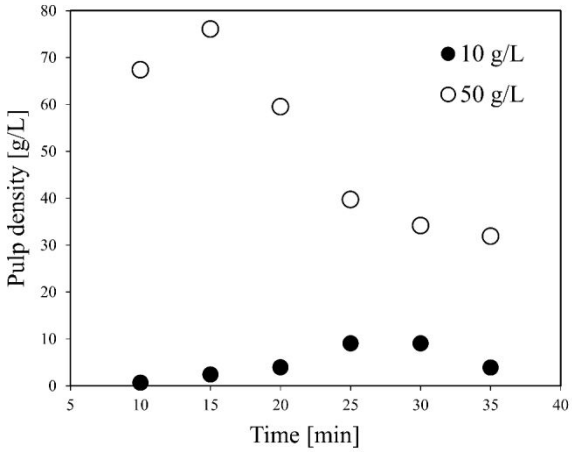

Fig. 1 Effect of time on pulp density of recovered solution using flow line A.

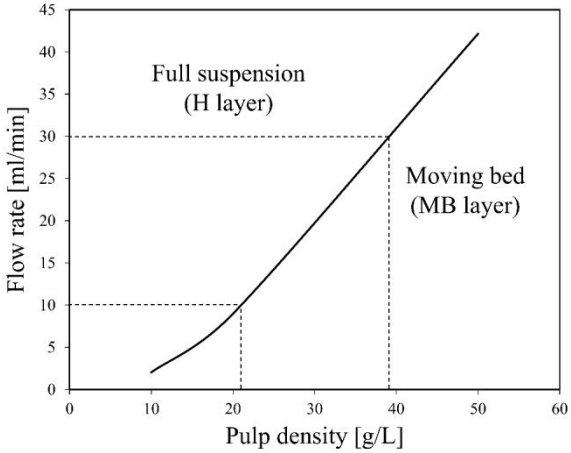

Fig. 2 Flow pattern map of $LiCoO_2$ slurry.

2.5 Analyses and definition

The size distribution of raw LIB material $LiCoO_2$ was obtained using a particle size analyzer (MT3300EXII, Microtrac). The composition of metal ions in the leachate was qualified and quantified by inductively coupled plasma atomic emission spectroscopy (ICP-AES; iCAP6500, Thermo Fisher), in which the wavelengths for identifying Li and Co, were 670 and 228 nm, respectively. Before the ICP test, the solution was diluted to 1/200.

Leaching efficiency was defined as the percentage of the mass of the metal ion in the recovered solution against the total mass of the metal ion in the starting material. The calculation equation (Equation 1) is shown as follows.

$$\text{Leaching efficiency} = \frac{Metal\ ion\ in\ \text{leachate}\ [g]}{Metal\ ion\ in\ feedstock\ [g]} \times 100\% \quad (1)$$

2.6 Three-layer model

In this study, a three-layer model was used to predict the characteristics of the solid-liquid flow (slurry flow). As supposed in the three-layer model and shown in **Scheme 4**,[31] when a solid-liquid mixture flows in a horizontal pipe at a flow rate, three layers exist in the pipe: a stationary bed (SB layer) at the bottom, a moving bed (MB layer) above it, and a heterogeneous suspended flow (H layer) at the top. The detailed formula derivation process follows a previous report,[32] and was described in **ESI**. Finally, a flow pattern map, which expresses the relationship between the pulp density and flow rate of $LiCoO_2$ slurry, was constructed and used to predict the flow state of the slurry and set the conditions under which accumulation or deposition does not occur.

3 Results and discussion

3.1 Cold flow test

The results of cold flow tests without heating were obtained to determine the conditions in the further continuous leaching experiments, mainly flow rate and pulp density.

3.1.1 Flow line A

Fig. 1 shows the effect of time on the pulp density of the recovered solution using flow line A at the flow rate of 10 ml/min. A higher initial pulp density is more possible to cause the accumulation of particles, and the variation of the pulp density of the recovered solution is usually regarded as one of the most important criteria to judge the occurrence of the accumulation. When an accumulation occurs, the pulp density of the recovered solution would go down first; along with the continuous injection of the slurry, the accumulated $LiCoO_2$ particles would be carried quickly after a critical point, like a dam burst, resulting in a rapid rise of the pulp density of the recovered solution. When the pulp density of the feeding slurry was 10 g/L, the recovered solution had a maximum of pulp density at around 10 g/L. Even though the pulp density of recovered solution dropped after 35 min, the results were enough to prove that a stable feeding was possible. On the other hand, when the pulp density of the feeding slurry was 50 g/L, the pulp density of the recovered solution was 30–80 g/L, showing a large variation. Particularly, the pulp density of the recovered solution at each time of 10, 20, and 30 min is higher than that of initial pulp density at 50 g/L. In addition, after completion of the experiment, the inside of the tube was washed and a large amount of $LiCoO_2$ particles were recovered. These evidences revealed an agglomeration of $LiCoO_2$ particles. It was speculated that the pumping became insufficient with increasing pulp density of the feeding slurry, simultaneously with the deposition of solid particles in the tube.

Fig. 2 shows the relationship between the pulp density and flow rate of $LiCoO_2$ slurry calculated using the three-layer model. The density of $LiCoO_2$ is 5000 kg/m^3, and the average particle size was 12.4 μm based on the particle size distribution shown in **Fig. S1**. The density (ρ_L) and viscosity (μ_L) of the H_3Cit aqueous solution were assumed to be similar to water. The viscosity of the slurry (μ_s) was assumed to be similar to water. In **Fig. 2**, the area above the solid line represents the full suspension area (H layer), where the liquid is flowing without forming a deposit, and the bottom area is the moving bed area (MB layer) that is transported while forming a deposit. From **Fig. 2**, it was found that at a flow rate of 10 ml/min, the slurry can be transferred without depositing when the pulp density was less than about 21 g/L, while at the pulp density of 50 g/L, $LiCoO_2$ particles can deposit in the tube, making a stable liquid transfer difficult. This

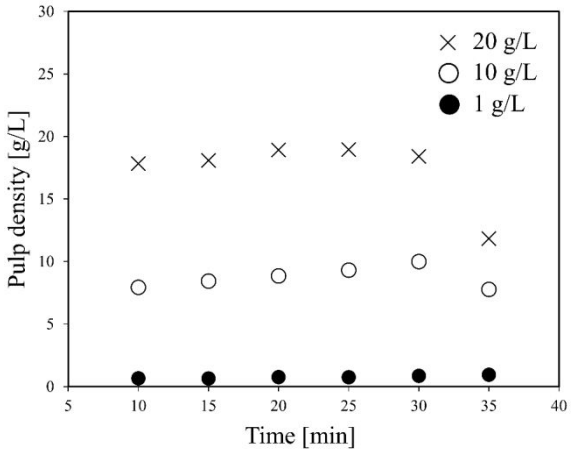

Fig. 3 Effect of time on pulp density of recovered solution using flow line B. ($LiCoO_2$, 30 ml/min)

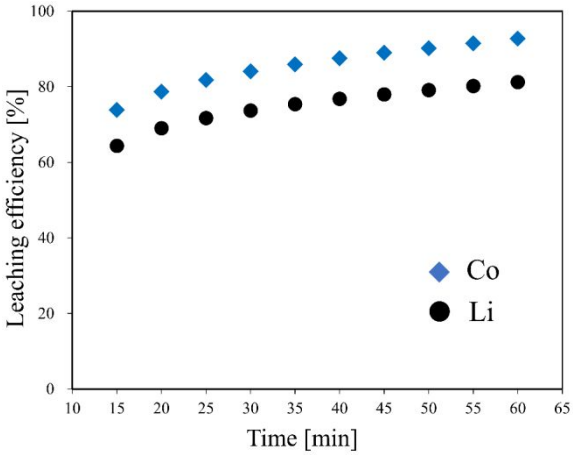

Fig. 4 Effect of time on leaching efficiency of Li and Co during the continuous hydrothermal leaching of $LiCoO_2$ with H_3Cit.

gave a good explanation of the experimental results shown in **Fig. 1**.

3.1.2 Flow line B

To get closer to the actual outline, the cold flow test using flow line B was described here. From the viewpoints of suppressing the deposition and improving the operability, the flow rate was increased from 10 to 30 ml/min. In addition, to suppress the accumulation further, the feeding tanks were moved at a higher position than the product collector, so that the flowing from the feeding tank to the product collector was not against gravity, and the pipe was arranged to go down gradually.

Fig. 3 shows the effect of time on the pulp density of the recovered solution using flow line B. When the pulp density of the slurry was 1 g/L, the recovered solution has a stable pulp density in each of six samplings. When the slurry pulp density increased to 10 or 20 g/L, the pulp density of the recovered solution was stable in the first five samplings, but then dropped in the 6th time. Especially at the slurry pulp density of 20 g/L, the pulp density of the recovered solution in the 6th sampling decreased a lot to almost a half. From **Fig. 2**, under the conditions of 10 or 20 g/L (pulp density of the feeding slurry) and 30 ml/min (flow rate), it is in the full suspension range and

Table 2 The concentration of each metal ion in the recovered solutions at different times during the continuous hydrothermal leaching of $LiCoO_2$ with H_3Cit. *

Time [min]	Li [ppm]	Co [ppm]	Ni [ppm]	Mn [ppm]	Fe [ppm]	Cr [ppm]
15	472.9	4553.2	103.7	7.9	301.0	85.5
20	528.1	5138.2	103.9	6.4	275.7	79.3
25	555.8	5358.5	109.0	6.1	258.6	77.1
30	573.0	5551.5	115.9	5.9	246.1	74.8
35	591.3	5682.3	120.2	5.8	240.8	73.6
40	596.7	5800.4	126.6	5.6	235.9	74.6
45	611.7	5899.4	131.4	5.4	230.8	75.1
50	638.9	6071.5	139.0	5.8	236.9	77.5
55	650.5	6255.9	148.0	5.8	235.8	78.0
60	666.0	6412.9	151.8	5.6	234.2	78.4

*: H_3Cit: 0.4 mol/L; flow rate: 30 ml/min.

accumulation should not occur. The confliction again illustrates the difference between the theoretical model results and the actual experimental results. A possible reason for the decrease in the 6th time is that particles accumulate in the slurry pump as time elapses from the start of the slurry feeding, and then the feeding performance is impaired. The $LiCoO_2$ particles might deposit in the slurry pump and cause blockage, thereby lowers the transfer rate. That is, it can be expected that a long-time operation will be difficult for this flow system when the pulp density of the slurry is high.

Based on the above results, the pulp density of the slurry and the flow rate were set to 10 g/L and 30 ml/min, respectively, in the next continuous hydrothermal acid leaching experiments.

3.2 Continuous hydrothermal leaching of $LiCoO_2$ with H_3Cit

As the most expensive LIB cathode material with a large market share, $LiCoO_2$ was chosen to be the research target of the first-time continuous hydrothermal leaching process. The conditions for the preliminary experiments were decided according to the results of the three-layer model and cold flow test.

Fig. 4 shows the leaching efficiency of Li and Co at different times during the continuous hydrothermal leaching of $LiCoO_2$ with H_3Cit (0.4 mol/L). At 15 min after the start of slurry feeding, which was the first sampling, the leaching efficiency of Li and Co were 64% and 74%, respectively. Then, the leaching efficiency of metals increased with the extension of time gradually, which can be attributed to that the replacement of the H_3Cit aqueous solution in the system with the slurry was insufficient immediately after the switching. At 60 min, which was the 10th sampling, the leaching efficiency of Li and Co achieved 81.3% and 92.7%, respectively, approach to the data obtained using a batch-style apparatus at 15 min.[26] Therefore, the recovered solution or leachate with a high leaching efficiency can be collected continuously since 60 min of feeding the slurry, even if the leaching efficiencies of Li and Co are expected to increase even after 60 min.

This is the first time to achieve continuous leaching of LIB cathode materials by the hydrothermal method. Even though the current condition may be far away from the optimum, the results are sufficient to prove the feasibility of the continuous hydrothermal leaching process and the applicability of this flow system.

Table 3 Elemental composition of stainless steel using in the flow system. *

	Ni [wt%]	Mn [wt%]	Fe [wt%]	Cr [wt%]
SUS304	8~11	<2	67~69	18~20
SUS316	10~14	<2	64~66	16~18

*: The steel types include SUS304 and SUS316.

3.3 Problem analysis during continuous hydrothermal leaching of $LiCoO_2$ with H_3Cit

As this is the first running of the flow system for hydrothermal leaching, the problems existed inevitably. Problem analysis is beneficial to the improvement of this technology. One of the most obvious problems is that metal ions other than Li and Co were analyzed from the recovered solution.

Table 2 shows the concentration of each metal ion in the recovered solutions at different times during hydrothermal leaching of $LiCoO_2$ with H_3Cit. Except for Li and Co, Ni, Fe, Cr, and a tiny amount of Mn, were detected. As pure $LiCoO_2$ compound was used in this study, the resource of other metal ions might be the steel materials used in the flow system. After comparing with the elemental composition of stainless steel used in the flow system, SUS306 and SUS3016, as listed in **Table 3**, it can be inferred that the other metal ions must originate from the steel tubes used in the flow system. Additionally, the variation trend of the concentration with the extension of time was different for different metal ions. With the extension of time, the concentration of Li, Co, and Ni increased, while that of Mn, Fe, and Cr decreased first and then tends to be unchanged. It is probably because at the beginning of the reaction, the H_3Cit corrodes the pipe and then the wall of the tube is 'protected' by the accumulation of $LiCoO_2$ as the reaction proceeds.

The acid corrosion revealed here is an obvious problem in the further application, but its severity is much lower than that caused by the use of inorganic acids or high-concentration organic acids in the conventional leaching method. It is known that the acids must be used in all current leaching processes. Even though the corrosion caused by the acids cannot be eliminated completely, its damage is being reduced gradually in the green progress. For example, there are several feasible ways to avoid or suppress acid corrosion. One is to coat Teflon or the materials with high acid corrosion resistance to the inner wall of the tubes. Another one is to choose the organic acids with low or no acid corrosion as the leachant. In addition, continuous manufacturing is an unavoidable step before the practical application. Therefore, this research is believed to be beneficial and significant to the sustainable development of continuous leaching of LIB cathode materials in the future.

Conclusions

The continuous hydrothermal leaching of $LiCoO_2$ with H_3Cit was successfully achieved using a specially designed and customized flow system. Prior to the hydrothermal acid leaching experiment, a three-layer model was used to predict the flow state in this flow system, and a cold flow test using two kinds of flow lines was performed to determine the conditions in the preliminary experiments. From the viewpoints of suppressing the deposition and improving the operability, the pulp density of the slurry and the flow rate were set to 10 g/L and 30 ml/min, respectively, and the position of feeding tanks was rearranged. In the first running of continuous hydrothermal leaching of $LiCoO_2$ with H_3Cit, the leaching efficiency of Li and Co reached 81.3% and 92.7%, respectively, at 60 min after the start of slurry feeding, and is expected to increase even after 60 min. It is promising to continuously obtain the recovered solution or leachate with a high leaching efficiency by continuing the operation, indicating a continuous hydrothermal leaching process is feasible and promising to be applied. Except for Li and Co, other metal ions were detected in the recovered solution, which was proven to be originated from the stainless steel used in the flow system. Meanwhile, the acid corrosion caused by H_3Cit was revealed, which is expected to be resolved by using the inner coating materials with high acid corrosion resistance or the organic acids with low or no acid corrosion as the leachant.

Conflicts of interest

There are no conflicts to declare.

Acknowledgements

This work was supported by the Japan Science and Technology Agency (JST)-Mirai program [grant number JP18077450] and the Japan Society for the Promotion of Science (JSPS)-Grant-in-Aid for challenging Exploratory Research [grant number No. 18K18966].

Notes and references

1. Y. Nishi, *J. Power Sources*, 2001, **100**, 101-106.
2. B. Scrosati, J. Hassoun and Y. K. Sun, *Energy Environ. Sci.*, 2011, **4**, 3287-3295.
3. W. Gao, J. Song, H. Cao, X. Lin, X. Zhang, X. Zheng, Y. Zhang and Z. Sun, *J. Clean. Prod.*, 2018, **178**, 833-845.
4. J. W. Fergus, *J. Power Sources*, 2010, **195**, 939-954.
5. C. Liu, J. Lin, H. Cao, Y. Zhang and Z. Sun, *J. Clean. Prod.*, 2019, **228**, 801-813.
6. M. K. Jha, A. Kumari, A. K. Jha, V. Kumar, J. Hait and B. D. Pandey, *Waste Manage. (Oxford)*, 2013, **33**, 1890-1897.
7. C. K. Lee and K.-I. Rhee, *J. Power Sources*, 2002, **109**, 17-21.
8. M. Chen, X. Ma, B. Chen, R. Arsenault, P. Karlson, N. Simon and Y. Wang, *Joule*, 2019, **3**, 2622-2646.
9. F. Gu, P. A. Summers and P. Hall, *J. Clean. Prod.*, 2019, **237**, 117657.
10. R. Golmohammadzadeh, F. Faraji and F. Rashchi, *Resources, Conservation and Recycling*, 2018, **136**, 418-435.
11. Q. Meng, Y. Zhang and P. Dong, *J. Clean. Prod.*, 2018, **180**, 64-70.
12. X. Chen, C. Luo, J. Zhang, J. Kong and T. Zhou, *ACS Sustain. Chem. Eng.*, 2015, **3**, 3104-3113.
13. X. Zheng, Z. Zhu, X. Lin, Y. Zhang, Y. He, H. Cao and Z. Sun, *Engineering*, 2018, **4**, 361-370.
14. D. A. Ferreira, L. M. Z. Prados, D. Majuste and M. B. Mansur, *J. Power Sources*, 2009, **187**, 238-246.

15. P. Meshram, Abhilash, B. D. Pandey, T. R. Mankhand and H. Deveci, *JOM*, 2016, **68**, 2613-2623.
16. L. Li, W. Qu, X. Zhang, J. Lu, R. Chen, F. Wu and K. Amine, *J. Power Sources*, 2015, **282**, 544-551.
17. L. Li, J. B. Dunn, X. X. Zhang, L. Gaines, R. J. Chen, F. Wu and K. Amine, *J. Power Sources*, 2013, **233**, 180-189.
18. L. Li, J. Ge, F. Wu, R. Chen, S. Chen and B. Wu, *J. Hazard. Mater.*, 2010, **176**, 288-293.
19. F. Meng, Q. Liu, R. Kim, J. Wang, G. Liu and A. Ghahreman, *Hydrometallurgy*, 2020, **191**, 105160.
20. G. P. Nayaka, J. Manjanna, K. V. Pai, R. Vadavi, S. J. Keny and V. S. Tripathi, *Hydrometallurgy*, 2015, **151**, 73-77.
21. S. Natarajan, A. B. Boricha and H. C. Bajaj, *Waste Manage. (Oxford)*, 2018, **77**, 455-465.
22. L. Li, E. Fan, Y. Guan, X. Zhang, Q. Xue, L. Wei, F. Wu and R. Chen, *ACS Sustain. Chem. Eng.*, 2017, **5**, 5224-5233.
23. L.-P. He, S.-Y. Sun, Y.-Y. Mu, X.-F. Song and J.-G. Yu, *ACS Sustain. Chem. Eng.*, 2017, **5**, 714-721.
24. X. Zeng, J. Li and B. Shen, *J. Hazard. Mater.*, 2015, **295**, 112-118.
25. G. P. Nayaka, K. V. Pai, G. Santhosh and J. Manjanna, *Journal of Environmental Chemical Engineering*, 2016, **4**, 2378-2383.
26. T. Aikawa, M. Watanabe, T. M. Aida and R. L. Smith Jr, *Kagaku Kogaku Ronbunshu*, 2017, **43**, 313-318.
27. L. Li, J. Lu, Y. Ren, X. X. Zhang, R. J. Chen, F. Wu and K. Amine, *J. Power Sources*, 2012, **218**, 21-27.
28. D. Azuma, T. Aikawa, Y. Hiraga, M. Watanabe and R. L. Smith Jr, *Kagaku Kogaku Ronbunshu*, 2019, **45**, 147-157.
29. G. S. Calabrese and S. Pissavini, *AlChE Journal*, 2011, **57**, 828-834.
30. L. Rogers and K. F. Jensen, *Green Chemistry*, 2019, **21**, 3481-3498.
31. P. Doron and D. Barnea, *Int. J. Multiphase Flow*, 1993, **19**, 1029-1043.
32. P. Doron, D. Granica and D. Barnea, *Int. J. Multiphase Flow*, 1987, **13**, 535-547.

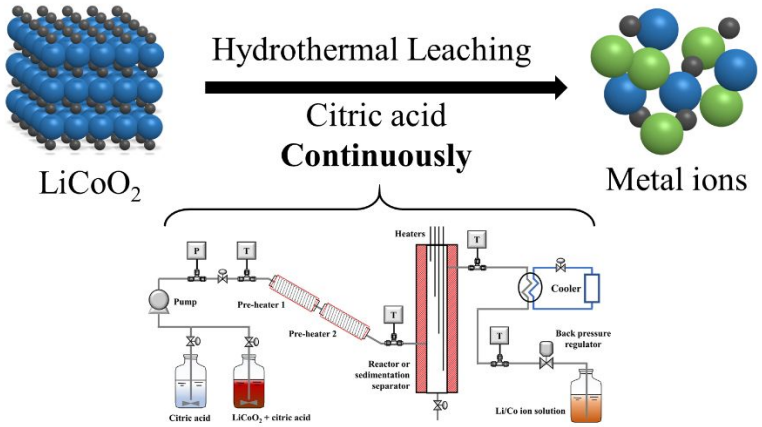

The continuous hydrothermal leaching of $LiCoO_2$ cathode materials with citric acid was firstly achieved using a customized flow system.